

## Peptidomimetic Inhibitors of Herpes Simplex Virus Ribonucleotide Reductase: A New Class of Antiviral Agents

Neil Moss,\* Pierre Beaulieu, Jean-Simon Duceppe, Jean-Marie Ferland, Jean Gauthier, Elise Ghiron, Sylvie Goulet, Louis Grenier, Montse Llinas-Brunet, Raymond Plante, Dominik Wernic, and Robert Déziel

Bio-Méga/Boehringer Ingelheim Research Inc., 2100 Cunard, Laval, Québec, Canada H7S 2G5

Received April 4, 1995\*

We have been investigating a new class of antiviral compounds effective against herpes simplex virus (HSV) *in vitro* and *in vivo*. Antiviral activity results from inhibition of HSV ribonucleotide reductase (RR). The inhibitors are designed as mimics of the RR small subunit C-terminus, a region essential for RR subunit association and consequently enzymatic activity. Inhibition results from specific binding of the inhibitor to the HSV RR large subunit thereby preventing subunit association. This report details the structure–activity studies that lead to the identification of BILD 1263, a potent inhibitor of HSV RR subunit association ( $IC_{50}$ , 0.2 nM) that also inhibits the replication of HSV types 1 and 2 in cell culture ( $EC_{50}$ , 3 and 4  $\mu$ M) and reduces the severity of HSV-1-induced keratitis in a murine ocular model. The discovery of inhibitors with *in vitro* antiviral activity results from a combination of improving inhibitor potency in a RR binding assay and modifying inhibitor physicochemical properties. The importance and possible role of the new structural modifications introduced into this inhibitor series is discussed.

### Introduction

The search for new therapeutics for herpes virus infections is an area of active investigation.<sup>1</sup> We recently introduced a new class of antiviral compounds effective against herpes simplex virus (HSV) *in vitro* and *in vivo*.<sup>2,3</sup> Antiviral activity resulted from inhibition of HSV ribonucleotide reductase (RR), the enzyme responsible for converting ribonucleoside diphosphates into the corresponding deoxynucleotides required for viral DNA biosynthesis.<sup>4</sup> The inhibitors were designed as mimics of the RR small subunit C-terminus, a region essential for RR subunit association and consequently enzymatic activity.<sup>5–8</sup> Inhibition resulted from specific binding of the inhibitor to the HSV RR large subunit thereby preventing subunit association. The highlighted compound in this paper, BILD 1263 (Table 3), was not only a potent inhibitor of RR subunit association but also inhibited the replication of HSV types 1 and 2 in cell culture ( $EC_{50}$  3 and 4  $\mu$ M, respectively). More significantly, this compound reduced the severity of HSV-1-induced keratitis in a murine ocular model.<sup>2</sup> In cell culture, BILD 1263 also strongly potentiated the antiviral activity of the most widely used antiherpetic drug, acyclovir, and was effective against acyclovir resistant HSV strains.<sup>2</sup> These results indicated the clinical potential of this type of antiviral strategy and provided an interesting example of a peptidomimetic compound that acts by preventing protein–protein interaction inside infected cells. Here we provide a detailed account of the structure–activity studies that lead to the discovery of BILD 1263. This study also provides insight into factors that influence the cell culture activity of these peptidomimetic inhibitors and provides evidence for how certain inhibitor functionalities contribute to binding potency.

Previous investigations showed that the first five to six C-terminal amino acids of peptides corresponding to the C-terminus of the HSV RR small subunit likely

constitute the minimum core for effective binding to the large subunit.<sup>9</sup> Structure activity studies by us<sup>10,11</sup> and others<sup>12</sup> employed C-terminal peptides (e.g., hexapeptide H-Ala-Val-Val-Asn-Asp-Leu-OH, compound 1, Table 1) as lead compounds to identify potent inhibitors of RR subunit association. Our first structure–activity paper introduced a series of substituted tetrapeptide derivatives culminating in compound 2a (Table 1).<sup>10</sup> The combination of replacing the appropriate N-terminal residues of the peptide leads with a diethylacetyl group, adding a methyl group to the adjacent valine, replacing the asparagine side-chain  $NH_2$  with a pyrrolidine, and substituting the  $\beta$ -hydrogens of the aspartic acid moiety with methyl groups afforded a derivative over 1000 times more potent than peptide 1. A systematic investigation of the structural requirements at each of the five amino acid positions in 2a also provided insight into how each side chain contributed to inhibitor potency. A subsequent investigation revealed that replacement of the  $\beta,\beta$ -dimethylaspartic acid residue in 2a with cyclopentylaspartic acid (compound 2b) produced a further 7-fold increase in binding potency.<sup>11</sup> Although 2b had an  $IC_{50}$  of 6 nM, it and the other derivatives revealed in these two papers proved ineffective at inhibiting the growth of either HSV-1 or -2 in cell culture at concentrations below 1000  $\mu$ M.

In order to be effective at preventing HSV replication, any RR subunit association inhibitor must penetrate inside infected cells. The uptake of peptidomimetics into cells has been an important issue in various peptide-based drug programs, the HIV protease field being a well-known example. Although to our knowledge no systematic investigation of factors affecting cell culture efficacy of HIV protease inhibitors has appeared in the literature, the following trends are evident. In general, the most effective HIV protease inhibitors in cell culture all appear to be potent inhibitors of the protease and are neutral or basic molecules.<sup>13</sup> One might expect acidic peptidomimetic derivatives such as

\* Abstract published in *Advance ACS Abstracts*, August 15, 1995.

Table 1

Compound	Binding Assay IC <sub>50</sub> (nM)
1	58,000 ± 14,000
2	43 ± 5 2a R = -CH <sub>3</sub> 2b R = -CH <sub>2</sub> (CH) <sub>2</sub> CH <sub>2</sub> -
3	860 ± 240
4	880 ± 300
5	24 ± 5

2, which contain two carboxylates at physiological pH, to have difficulty crossing a cell's lipid bilayer by passive diffusion. In order to address the lack of tissue culture activity of compounds such as 2, it became clear that we would have to experiment with inhibitor physicochemical properties. However, experiments aimed at further improving inhibitor binding potency provided the first breakthrough in HSV cell culture.

## Results and Discussion

(a) **Evaluation of Inhibitors in an RR Binding Assay<sup>14</sup> (IC<sub>50</sub>) and an HSV Cell Culture Assay (EC<sub>50</sub>).** The highlighted compounds from our two previous structure-activity papers contain a diethyl-acetyl group as a replacement for valine at the inhibitor N-terminus.<sup>10,11</sup> The similar potencies of compounds 3 and 4 (Table 1) illustrate the suitability of this diethyl-acetyl N-terminus as a replacement for the more peptidic *N*-acetylvaline residue. A survey of other *N*-terminal acyl groups that could replace the *N*-acetyl in compound 4 identified the 3-phenylpropionyl group as a superior substitution (compound 5). In fact the larger inhibitor series, represented by compound 5, has over 30 times greater potency than our previously published inhibitor series, represented by compound 3. Table 2 uses compound 5 as a point of reference and lists what we have so far found to be the optimal substitution for binding potency at each position. Compounds 6–12 illustrate the effect of single modifications to compound

Table 2

Compound	Binding Assay IC <sub>50</sub> (nM)
5	24 ± 5
6	0.7 ± 0.1
7	7.5 ± 1.3
8	4 ± 1
9	4000 ± 1100
10	1 ± 0.5
11	5 ± 1
12	34 ± 5

5. The previously reported<sup>10,11</sup> beneficial substitutions at the four C-terminal amino acid positions (Val-Asn-Asp-Leu) also improve the binding potency of this new inhibitor series (compounds 5, 8, 10, and 11). Table 2 also illustrates two further modifications that improve binding potency—addition of a second benzyl group to the N-terminus and methylation of the N-terminal amide (compounds 6 and 7). The role and beneficial effect of the extra benzyl group and the *N*-methylvaline moiety will be discussed in greater detail later.

The modifications depicted in compounds 6 and 10 individually improve the binding potency of compound 5 to the 1 nM level. Despite the potency of 6 and 10, these compounds and the others in Table 2 still did not inhibit the replication of HSV in cell culture below 1000 μM. However, incorporating all the best modifications into the same molecule produced a compound that inhibited the growth of both HSV-1 and HSV-2 in cell culture (BILD 1257, EC<sub>50</sub> 35 and 30 μM, respectively, Table 3). This compound achieved efficacious concentrations inside HSV-infected cells despite its high molecular weight (MW = 931) and polar, peptidic nature. The intrinsic binding potency of BILD 1257 may be an important factor contributing to its cell culture efficacy. BILD 1257 has an observed binding assay potency of 0.2 nM, which approaches the theoretical minimum IC<sub>50</sub> in this assay. The enzyme concentration in the binding assay is estimated to be approximately 0.2 nM, conse-

Table 3

Compound	Cell Culture Assay EC <sub>50</sub> (μM)	
	HSV-1	HSV-2
BILD 1257	35 ± 2	30 ± 4
BILD 1263	3.1 ± 0.4	4.2 ± 1.0
BILD 733	52 ± 9	35 ± 8
13	12 ± 4	14 ± 4
14	7 ± 1	6.5 ± 1.2
15	150 ± 10	150 ± 10
16	30 ± 4	39 ± 5
17	7.3 ± 1.5	7.3 ± 1

quently observed potencies of 1 nM or lower may not accurately reflect true inhibitor binding potency. Our previous structure–activity studies demonstrate that modifications to any of the four C-terminal amino acid side chains usually do not adversely influence the effect of adjacent beneficial substitutions. Thus, if one assumes a cumulative effect on binding potency of incorporating each of the five beneficial modifications contained in compounds **6**, **7**, **8**, **10**, and **11** into compound **5**, BILD 1257 would have a predicted binding potency of approximately 0.001 nM.

In addition to a relationship between inhibitor binding potency and cell culture potency, we also observe a relationship between certain inhibitor physicochemical properties and cell culture potency. A modification of the inhibitor C-terminus provides a clear illustration of this relationship. Replacing the C-terminal carboxylic acid in BILD 1257 with a hydroxymethyl group (BILD 1263, Table 3) improves cell culture potency approximately 10-fold. This hydroxymethyl group improves inhibitor tissue culture potency even though it binds less efficiently to the large subunit. Although our binding assay is not sensitive enough to accurately determine the IC<sub>50</sub>s of BILDs 1263 and 1257, a comparison of compounds **11** and **12** (Table 2) plus a previously published comparison<sup>10</sup> indicates that replacing the C-terminal carboxyl with a hydroxymethyl results in an

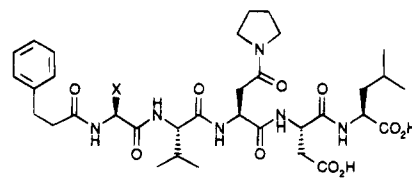
approximately 7-fold loss of binding potency. The reduced hydrophilicity of the hydroxymethyl group in BILD 1263 is evidently beneficial for cell culture potency and more than compensates for a small decrease in binding potency. It is noteworthy that a similar modification of the aspartic acid carboxyl group is not fruitful since this group contributes far more to inhibitor binding potency than the C-terminal carboxyl group.<sup>10</sup>






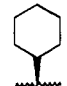
Although the modifications in Table 2 were designed to optimize inhibitor binding potency, it turns out that these modifications also contribute positively to the cell culture potency of BILD 1263. Table 3 illustrates the effect on cell culture potency of systematically replacing each of the beneficial binding modifications in BILD 1263 with the corresponding unmodified moiety (compounds **13**–**17** and BILD 733).<sup>15</sup> The various binding modifications contribute between 2 and 50 times to the cell culture potency of BILD 1263. In general, the modifications that have the largest effect on binding potency also have the greatest effect on tissue culture potency. However, all of these modifications also affect inhibitor physicochemical properties in a similar manner; that is, they are all lipophilic. It is conceivable that the lipophilicity of each modification may improve the ability of BILD 1263 to achieve efficacious concentrations inside the cell, thus contributing at least in part to cell culture potency. From the results presented so far, the intrinsic potency of the inhibitor and its physicochemical properties likely both play a significant role in defining inhibitor cell culture potency.

**(b) How Various Inhibitor Functionalities Contribute to Binding Potency.** Our previously published structure–activity studies provide hypotheses of how the amino acid side-chain functionalities at the first, second, and fourth position from the C-terminus (Leu, Asp, and Val in C-terminal sequence) contribute to inhibitor binding potency.<sup>10,11</sup> The isopropyl group of the C-terminal leucine residue (see compound **3**, Table 1) likely binds to a lipophilic pocket on the large subunit, since removing this group lowers inhibitor potency over 1000 times (i.e., inhibitor inactive at 1000 μM). The aspartic acid carboxyl group proves equally critical for inhibitor potency, thus implicating it in an important hydrogen-bonding interaction. Reference 11 provides detailed evidence that the cyclopentane ring on the aspartic acid residue found in compound **2b** serves to favor the binding conformation of the aspartic acid carboxyl. The *tert*-butyl side chain at the fourth amino acid position does not appear to interact directly with the large subunit but instead probably favors local inhibitor bioactive conformation. The role of the functionality at the third amino acid position (asparagine modified with a pyrrolidine) is not as evident as the roles of the other side-chain functionalities.

Our previous structure–activity studies also show that the N-terminal diethylacetyl group in a close analog of compound **3** likely participates in a lipophilic binding interaction with the large subunit, since truncation to an acetyl group severely lowers inhibitory potency in the binding assay (compound inactive at 1000 μM). Since the current inhibitor series has a significantly different N-terminus to the older series, we investigated the importance of the N-terminal valine side chain for inhibitor binding potency. Systematic truncation of the valine isopropyl group in compound **5** (Table 4) to a

Table 4



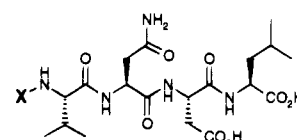
Compound	X	Binding Assay IC <sub>50</sub> (nM)
5		24 ± 5
18		340 ± 130
19		8800 ± 1200
20	H	115,000 ± 27,000
21		61 ± 9
22		36 ± 4
23		22 ± 4

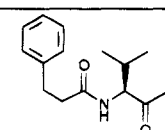
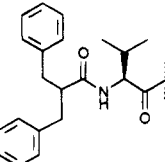
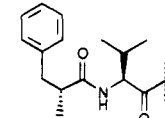
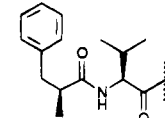
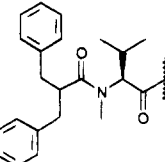
hydrogen (compounds **18–20**) culminates in an approximately 5000-fold loss of binding potency. This result further supports the importance of a lipophilic group at this position for optimal binding to the large subunit. The similar potencies of compounds **5**, **21**, **22**, and **23** suggest that the shape of the lipophilic group is not critical for optimal binding potency.

The N-terminus (phenylpropionyl or dibenzylacetyl group) of this new inhibitor series is a unique feature in that it has little structural similarity to the corresponding amino acid found in the RR small subunit C-terminus. The five C-terminal amino acid derivatives in BILD 1263 still resemble the corresponding amino acids found in the small subunit C-terminus (Val-Val-Asn-Asp-Leu), even though each position in BILD 1263 has been modified to improve binding and cell culture potency. However the N-terminus of BILD 1263 clearly has little structural similarity to the sixth and seventh amino acids found in the small subunit C-terminus (alanine and glycine, respectively). It appears that this new inhibitor series takes advantage of a binding site not used by the small subunit C-terminus.

On the basis of the difference in potency between compounds **4** and **5** (Table 1), we hypothesized that the benzyl group in **5** may be involved in a binding interaction with the large subunit, since it seemed unlikely that this remote group would significantly affect inhibitor conformation. A comparison between compounds **5** and **6** (Table 2) reveals that addition of a second benzyl group to the inhibitor N-terminus increases binding potency at least 25-fold.<sup>16</sup> However, since the potency of compound **6** approached the limit of sensitivity of our binding assay, we investigated the effect of the second benzyl group in a less potent inhibitor series to be sure of the exact magnitude of the potency increase. Com-

Table 5



Compound	X	Binding Assay IC <sub>50</sub> (nM)
9		4000 ± 1100
24		180 ± 30
25		860 ± 120
26		11000 ± 1000
27		22 ± 2

pounds **9** and **24** (Table 5) show a 22-fold difference in potency, thus confirming the relative contribution of the second benzyl group to binding potency. A comparison between compound **9** and compounds **24–26** (Table 5) suggest a possible role for the second benzyl group. Adding a stereochemically defined methyl group to the phenylpropionyl moiety in compound **9** improves activity in the case of the *R*-configuration (compound **25**) but decreases activity slightly in the case of the *S*-configuration (compound **26**). The similar binding potencies of inhibitors **24** and **25** suggest that the second benzyl group does not directly interact with the large subunit but instead favors a conformation of the inhibitor N-terminus that facilitates binding of the other benzyl group. The methyl group in **26** presumably favors conformations of the inhibitor N-terminus in which the benzyl group is not optimally oriented for binding to the large subunit.

An additional structural feature of this inhibitor series that requires further discussion is the methyl group on the N-terminal valine nitrogen (*cf.* compounds **5** and **7**, Table 2; compounds **24** and **27**, Table 5). The magnitude of potency enhancement obtained on methylating the valine nitrogen depends on the structure of the N-terminal acyl group. For inhibitors with an N-terminal phenylpropionyl group (compounds **5** and **7**), we observe a 3-fold increase in potency. However, for inhibitors with a N-terminal dibenzylacetyl group (compounds **24** and **27**), we observe a more substantial 8-fold increase in potency. The *N*-methyl group may be favorably influencing the conformation of the inhibitor

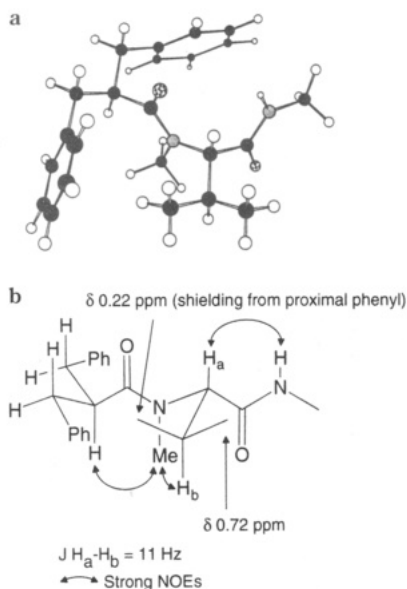


Figure 1.

N-terminal region. A combination of NMR data and molecular mechanics calculations helps suggest a possible three-dimensional structure for this region of the inhibitor. Figure 1a shows the lowest energy conformation resulting from a Monte Carlo conformational search of dibenzylacetyl-*N*-methylvaline methylamide, the N-terminal portion of our best inhibitors. A combination of NMR chemical shift, coupling constant, and NOE data obtained for BILD 1263 provides support that this conformation of the N-terminus also predominates in solution (see Figure 1b for relevant NMR data). On the basis of the structures in Figure 1 and the structure-activity study in Table 5 (compounds **25** and **26**), the binding benzyl group is situated in the same general direction as the valine isopropyl group. The valine *N*-methyl points away from the binding benzyl and isopropyl groups, suggesting that it may not be involved in a direct binding interaction. The *N*-methyl group may favor the N-terminal region's preferred geometry for binding and/or help reduce conformational mobility in this region of the inhibitor. The effect of the *N*-methyl group appears to be more pronounced in the presence of the second benzyl, a group that also influences the conformation of the inhibitor N-terminal region.

The comparison between compounds **4** and **5** illustrates that addition of a benzyl group to the inhibitor N-terminus improves binding potency 36-fold. The comparison between compounds **9** and **27** indicates that favoring the bioactive conformation of the inhibitor N-terminus can improve binding potency a further 200-fold. These results provide an illustration of the potency gains obtainable by rigidifying conformationally flexible inhibitors. As mentioned previously, other groups in our inhibitors also act by favoring local inhibitor bioactive conformation. Figure 2 provides a summary of what we currently believe to be the role of the various functionality in BILD 1263. Four individual groups are so far implicated in direct binding interactions with the RR large subunit and four groups are implicated in favoring local inhibitor bioactive conformation.

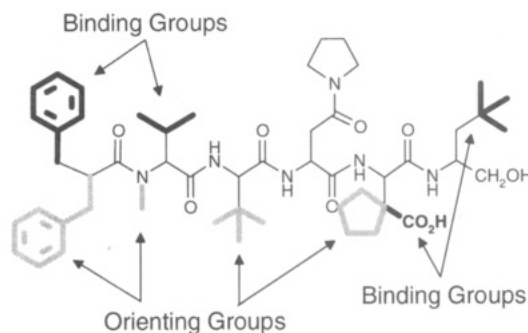


Figure 2.

## Conclusion

This report illustrated the structure-activity studies that lead to the discovery BILD 1263, the first reported ribonucleotide reductase subunit association inhibitor to possess antiviral activity *in vivo*. We detailed the importance of various structural modifications for inhibition of RR subunit association and for inhibition of HSV-1 and -2 replication in cell culture. These results highlighted the relationship between inhibitor binding potency, physicochemical properties, and cell culture potency. The presence of a well-oriented benzyl group at the N-terminus of this inhibitor series improves binding potency approximately 7000-fold over our previously published inhibitor series. This finding likely plays a significant role in the general antiviral properties of BILD 1263.

## Experimental Section

**Ribonucleotide Reductase Binding Assay.** The inhibitory effect of our compounds in an HSV ribonucleotide reductase radioligand binding assay was measured according to a published protocol.<sup>14</sup> The reported IC<sub>50</sub> values are the mean of at least four separate determinations, and the standard deviation from the mean is also reported.

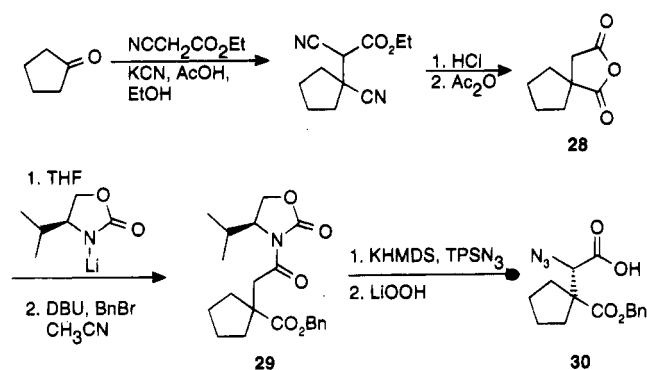
**HSV Cell Culture Assay.** The potencies of our inhibitors against HSV in cell culture were determined by using serum-starved baby hamster kidney (BHK) cells in a colorimetric viral yield assay.<sup>17</sup> The reported EC<sub>50</sub> values are the mean of at least three separate determinations, and the standard deviation from the mean is also reported. To confirm that the observed antiviral effect was not a consequence of cytotoxicity, the cytotoxic effect of all inhibitors was determined by a tetrazolium salt (MTT) metabolic assay.<sup>18</sup> Typically, selectivity indices (EC<sub>50</sub> versus CC<sub>50</sub>) of 15 or greater were observed for compounds having cell culture EC<sub>50</sub>s lower than 50  $\mu$ M. All compounds referred to in this paper proved stable under the assay conditions.

**Molecular Mechanics Calculations.** Dibenzylacetyl-*N*-methylvaline methylamide was subjected to a Monte Carlo conformational search. A total of 2500 generated structures were minimized (Polak-Ribier conjugate gradient method, 2000 iterations) with the MM3 force field as implemented in MacroModel v4.0. A dielectric constant of 80 was used to lessen the contribution of intramolecular hydrogen bonds. The conformation shown in Figure 1a is a Chem3D representation of the minimum energy conformation found from this search.

**Materials.** Common *N*-Boc-L-amino acids, *N*-Boc-*L*-tert-leucine, *N*-Boc-*L*- $\gamma$ -methylleucine, *L*-leucinol, and *N*-Boc-*N*-methyl-*L*-valine, were obtained from commercial sources. *N*-Boc-*L*- $\gamma$ -methylleucinol and Boc-2(*S*)-amino-4-pyrrolidino-4-oxobutanoic acid were obtained as outlined in ref 10. 2(*R*)- and 2(*S*)-methyl-3-phenylpropionic acid<sup>19</sup> and dibenzylacetic acid<sup>20</sup> were prepared according to literature procedures.

The synthesis of (*S*)- $\alpha$ -azido-1-(benzyloxycarbonyl)cyclopentaneacetic acid (**30**) (the precursor for the cyclopentylaspartic acid moiety) is outlined as follows (Scheme 1). The preparation of anhydride **28** is described in the literature.<sup>21</sup> (4*S*)-(-)-4-

## Scheme 1



Isopropyl-2-oxazolidinone (155 g, 1.2 mol) was dissolved in dry THF (1.4 L), and the resultant solution was mechanically stirred at  $-40^{\circ}\text{C}$  under an argon atmosphere. *n*-BuLi (2.5 M in hexane, 483 mL, 1.2 mol) was added dropwise to this solution, and the resultant slurry was stirred for 30 min at  $-40^{\circ}\text{C}$ . The reaction mixture was then cooled to  $-75^{\circ}\text{C}$ , and a solution of anhydride **28** (185 g, 1.2 mol) in THF (400 mL) was added dropwise. After addition, the cooling bath was removed and the internal temperature was allowed to increase to  $0^{\circ}\text{C}$ . Once at  $0^{\circ}\text{C}$ , the reaction temperature was maintained with an ice bath for 1 h. The clear yellow reaction mixture was treated with 10% aqueous citric acid (1 L). The organic phase was separated, and the aqueous phase was extracted three times with ethyl acetate. The combined extracts and organic phase were washed with brine, dried ( $\text{MgSO}_4$ ), and concentrated under reduced pressure to give a yellow oil which solidified on standing under vacuum (341 g, 100% yield). This material (340 g, 1.2 mol) was dissolved in acetonitrile (1.2 L), and the resultant solution was cooled to  $0^{\circ}\text{C}$ . Benzyl bromide (205 g, 1.2 mol) and 1,8-diazabicyclo[5.4.0]undec-7-ene (183 g, 1.2 mol) were added in one portion, the ice bath was removed, and the mixture was stirred at ambient temperature for 48 h. After removal of volatiles under reduced pressure, the residue was partitioned between water and ethyl acetate. The organic phase was washed with 10% aqueous citric acid and brine, dried ( $\text{MgSO}_4$ ), and concentrated. The resultant red oil was diluted with hexane, mixed with flash-grade silica gel (300 g), and dried under reduced pressure. The pink solid was added to a 2 L sintered-glass funnel, and the product was eluted from the silica gel with hexane (2 L) followed by 8:2 hexane-ethyl acetate (2 L). Concentration and crystallization of the residue from hot ethyl acetate-hexane gave compound **29** as a white solid (299 g, 67% yield): mp  $60-61^{\circ}\text{C}$ ;  $[\alpha]_D^{25} +59.1^{\circ}$  (*c* 1.00, EtOH);  $^1\text{H}$  NMR (400 MHz,  $\text{CDCl}_3$ )  $\delta$  7.37–7.26 (m, 5 H), 5.12 (s, 2 H), 4.32 (ddd, *J* = 8, 4, 4 Hz, 1 H), 4.22–4.14 (m, 2 H), 3.35 (s, 2 H), 2.25–2.20 (m, 3 H), 1.80–1.53 (m, 6 H), 0.86 (d, *J* = 7 Hz, 3 H), 0.80 (d, *J* = 7 Hz, 3 H);  $^{13}\text{C}$  NMR (100.6 MHz,  $\text{CDCl}_3$ )  $\delta$  176.7, 171.3, 154.0, 136.3, 128.3, 127.8, 66.2, 63.4, 58.2, 50.3, 44.6, 36.9, 36.8, 28.3, 25.4, 17.7, 14.5; EI-MS exact mass calcd for  $\text{C}_{21}\text{H}_{27}\text{NO}_5$  373.1889, found 373.1847. Anal. Calcd for  $\text{C}_{21}\text{H}_{27}\text{NO}_5$ : C, 67.54; H, 7.28; N, 3.75. Found: C, 67.56; H, 7.35; N, 3.66.

A solution of compound **29** (150 g, 0.401 mol) in dry THF (450 mL) was added to an addition funnel equipped with a cooling jacket maintained at  $-75^{\circ}\text{C}$ . This solution was added dropwise over a period of 20 min to a solution of KHMDS (0.692 M in THF, 586 mL, 0.405 mol) in THF (200 mL) at  $-75^{\circ}\text{C}$  under an argon atmosphere. After 45 min, a solution of 2,4,6-trisopropylbenzenesulfonyl azide (143 g, 0.462 mol) in THF (200 mL), also at  $-75^{\circ}\text{C}$  in a cooled addition funnel, was added rapidly in one portion. After 2 min, the reaction was treated with glacial acetic acid (150 mL) and was allowed to warm up to room temperature. The reaction flask was immersed in a warm bath ( $35-40^{\circ}\text{C}$ ) for 1 h. The THF was removed under reduced pressure, and the yellow pasty residue was titrated with 8:2 hexane-ethyl acetate (3 L). The precipitated 2,4,6-trisopropylbenzenesulfonic acid was removed by filtration, and the filtrate was concentrated to give an orange oil. This material was diluted with hexane, mixed

with flash-grade silica gel (600 mL), and concentrated/dried at  $40^{\circ}\text{C}$  using a rotary evaporator for 20 h. The resultant material was loaded on a flash silica chromatography column (15  $\times$  23 cm) and eluted successively with hexane, 95:5 hexane-ethyl acetate, and 9:1 hexane-ethyl acetate to give the desired product as a yellow oil (131 g, 78% yield):  $[\alpha]_D^{25} -34.7^{\circ}$  (*c* 1.00 MeOH);  $^1\text{H}$  NMR (400 MHz,  $\text{CDCl}_3$ )  $\delta$  7.39–7.28 (m, 5 H), 5.72 (s, 1 H), 5.22 (d, *J* = 12.5 Hz, 1 H), 4.94 (d, *J* = 12.5 Hz, 1 H), 4.18–4.00 (m, 3 H), 2.38–2.20 (m, 2 H), 2.07–1.66 (m, 7 H), 0.87 (d, *J* = 7 Hz, 3 H), 0.86 (d, *J* = 7 Hz, 3 H);  $^{13}\text{C}$  NMR (100.6 MHz,  $\text{CDCl}_3$ )  $\delta$  175.5, 168.4, 153.5, 135.6, 128.4, 128.1, 127.9, 66.4, 64.2, 63.5, 58.1, 55.6, 36.8, 31.5, 28.1, 26.9, 25.6, 17.6, 14.4; EI-MS exact mass calcd for  $\text{C}_{21}\text{H}_{26}\text{N}_2\text{O}_5$  (M – N<sub>2</sub>) 386.1841, found 386.1865.

The product from the previous reaction (112 g, 270 mmol) was dissolved in 3:1 THF-water (5.9 L) and the solution was cooled to  $0^{\circ}\text{C}$ . Hydrogen peroxide (30%, 138 mL, 1.22 mol) was added followed by lithium hydroxide monohydrate (23.8 g, 567 mmol). The reaction mixture was stirred vigorously for 9 min and was then treated with a solution of sodium sulfite (256 g, 2.03 mol) in water (1.5 L) and sodium bicarbonate (18 g, 0.21 mol). The THF was removed under reduced pressure, and the resultant aqueous solution was extracted continuously with chloroform for 20 h to remove the chiral auxiliary. The chloroform layer was concentrated, the residue redissolved in 10% aqueous sodium bicarbonate, and the solution reextracted continuously with chloroform. The aqueous phases from the two extractions were combined, cooled in ice, and acidified to pH 2 with concentrated HCl. The acidified solution was extracted with ethyl acetate, and the organic phase was washed with brine, dried ( $\text{MgSO}_4$ ), and concentrated to give azide **30** as a clear oil which solidified *in vacuo* (80.8 g, 98% yield). This material was of sufficient purity for coupling to an appropriate C-terminal residue. An analytical sample could be obtained by reverse phase HPLC (Whatman partisil 10 ODS-3 column, eluent 0–60% acetonitrile in water, both solvents containing 0.06% TFA), followed by lyophilization. The resultant residue was dissolved in ether and concentrated to provide, after drying *in vacuo*, compound **30** as a white solid: mp  $55-56^{\circ}\text{C}$ ;  $[\alpha]_D^{25} -93.5^{\circ}$  (*c* 1.00, MeOH);  $^1\text{H}$  NMR (400 MHz,  $\text{CDCl}_3$ )  $\delta$  7.40–7.30 (m, 5 H), 5.17 (d, *J* = 12.5 Hz, 1 H), 5.13 (d, *J* = 12.5 Hz, 1 H), 4.52 (s, 1 H), 2.30–2.20 (m, 1 H), 2.03–1.97 (m, 2 H), 1.79–1.62 (m, 7 H);  $^{13}\text{C}$  NMR (100.6 MHz,  $\text{CDCl}_3$ )  $\delta$  174.9, 174.8, 135.4, 128.5, 128.3, 128.1, 67.1, 66.8, 55.8, 35.7, 31.9, 26.0, 25.8; FAB-MS exact mass calcd for  $\text{C}_{15}\text{H}_{17}\text{N}_3\text{O}_4$  304.1297, found 304.1270. Anal. Calcd for  $\text{C}_{15}\text{H}_{17}\text{N}_3\text{O}_4$ : C, 59.39; H, 5.65; N, 13.85. Found: C, 59.16; H, 5.61; N, 13.82. The enantiomeric purity was assessed by conversion of **30** to the dibenzyl ester of cyclopentylaspartic acid (DBU, benzyl bromide, and  $\text{CH}_3\text{CN}$  followed by  $\text{SnCl}_2$ , MeOH) and subjection of this compound to chiral HPLC analysis (Chiracel OD column, eluent: 5% ethanol in hexane). Comparison of the derivative obtained from compound **30** with the corresponding racemic counterpart<sup>11</sup> indicated 3–6% enantiomeric contamination.

**Inhibitor Synthesis.** All inhibitors were prepared by solution phase peptide synthesis, in which *N*-Boc-amino acid derivatives were coupled sequentially from C- to N-terminus by using benzotriazol-1-yl-1,1,3,3-tetramethyluronium tetrafluoroborate (TBTU) as the coupling agent, and subsequent removal of the *N*-Boc protective group was effected by 4 N HCl in dioxane. The following procedure is representative. To a solution of *N*-Boc-amino (1 mmol) in dry acetonitrile (2.5 mL) was added TBTU (1 mmol) and *N*-methylmorpholine (1 mmol). After approximately 5 min, this solution was added to a solution of amino acid or peptide hydrochloride salt (1 mmol) in dry acetonitrile (2.5 mL) containing *N*-methylmorpholine (2 mmol). The reaction mixture was stirred at ambient temperature for 2–6 h (reaction monitored by TLC) and then poured into a mixture of ethyl acetate (50 mL) and saturated aqueous sodium bicarbonate (50 mL). The organic phase was washed with another portion of sodium bicarbonate, 1 N aqueous HCl (2  $\times$  50 mL), and brine (50 mL). Drying ( $\text{MgSO}_4$ ), filtration, and concentration provided the peptide, usually of sufficient purity to continue to the next step without further purification. *N*-Boc peptide derivatives could be purified if



necessary by conventional flash chromatography. The *N*-Boc-peptide product (1 mmol) was then treated with 4 N HCl in dioxane (5 mL) for 30 min. The solvent was removed under vacuum, and the resulting hydrochloride salt was subjected to high vacuum before its use in the next coupling reaction. Coupling of the *N*-terminal acyl groups was accomplished via the acid chloride (generated from the corresponding carboxylic acid by standard protocols) in acetonitrile containing 1 equiv of *N*-methylmorpholine. The cyclopentylaspartic acid moiety was incorporated as the azido derivative **30**. After coupling to the appropriate C-terminal residue, the azido group was reduced to the corresponding amine according to literature procedure.<sup>22</sup> At this point the small quantities of diastereomeric material containing D-cyclopentylaspartic acid could be readily removed by silica gel flash chromatography.

Subsequently, the fully protected peptide derivatives were purified by flash chromatography, and the various benzyl-related protective groups were removed by catalytic hydrogenolysis by using 10% Pd/C (10 mol %) in methanol and 1 atm of H<sub>2</sub> for 3 h. The resultant inhibitor was usually obtained in greater than 95% purity (HPLC and NMR), but if necessary it could be purified by preparative HPLC on a C18 reverse-phase column (Vydac, 15  $\mu$ m particle size) eluting with 0.06% aqueous TFA–0.06% TFA in acetonitrile gradients.

**Inhibitor Characterization and Purity.** All peptide derivatives showed satisfactory 400 MHz <sup>1</sup>H NMR spectra, FAB mass spectra (M<sup>+</sup> + H) and/or (M<sup>+</sup> + Na), amino acid analysis including peptide recovery, and HPLC purity in two solvent systems (>95%). Satisfactory elemental analyses were obtained for BILD 1263 and 1257 based on water content determined by Karl-Fischer titration.

**Acknowledgment.** We are grateful to M. Liuzzi and E. Scouten for determining the IC<sub>50</sub>s of our inhibitors in the binding assay. We are also grateful C. Bousquet and N. Dansereau for determining EC<sub>50</sub>s of our inhibitors in cell culture.

**Supporting Information Available:** Full tabulation of <sup>1</sup>H NMR, FAB mass spectra, amino acid analysis, elemental analysis, and HPLC purity data for new inhibitors (10 pages). Ordering information is given on any current masthead page.

## References

- (1) *Antiviral chemotherapy. New directions for clinical application and research*; Mills, J., Cory, L., Eds.; PTR Prentice Hall: Englewood Cliffs, NJ, 1993; Vol. 3.
- (2) Liuzzi, M.; Déziel, R.; Moss, N.; Beaulieu, P.; Bonneau, A.-M.; Bousquet, C.; Chafouleas, J. G.; Garneau, M.; Jaramillo, J.; Krogsrud, R. L.; Lagacé, L.; McCollum, R. S.; Nawoot, S.; Guindon, Y. A potent peptidomimetic inhibitor of HSV ribonucleotide reductase with antiviral activity *in vivo*. *Nature* **1994**, *372*, 695–698.
- (3) For a preliminary account of antiviral activity *in vitro*, see: Moss, N.; Déziel, R.; Beaulieu, P.; Bonneau, A.-M.; Krogsrud, R. L.; Liuzzi, M.; Plante, R.; Guindon, Y. *Peptides: Chemistry and Biology. Proceedings of the Thirteenth American Peptide Symposium*; Hodges, R. S., Smith, J. A., Eds.; Escom: Leiden, 1993; pp 580–582.
- (4) Cory, J. G. Role of ribonucleotide reductase in cell division. In *Inhibitors of Ribonucleoside Diphosphate Reductase Activity*; Cory, J. G., Cory, A. H., Eds.; Pergamon Press Inc.: New York, 1989; pp 1–17.
- (5) Dutia, B. M.; Frame, M. C.; Subak-Sharpe, J. H.; Clarke, W. N.; Marsden, H. S. Specific inhibition of herpes virus ribonucleotide reductase by synthetic peptides. *Nature* **1986**, *321*, 439–441.
- (6) Cohen, E. A.; Gaudreau, P.; Brazeau, P.; Langelier, Y. Specific inhibition of herpes simplex virus ribonucleotide reductase activity by a nonapeptide derived from the carboxyl terminus of subunit 2. *Nature* **1986**, *321*, 441–443.
- (7) Cosentino, G.; Lavallée, P.; Rakhit, S.; Plante, R.; Gaudette, Y.; Lawetz, C.; Whitehead, P. W.; Ducepe, J.-S.; Lépine-Frenette, C.; Dansereau, N.; Guilbault, C.; Langelier, Y.; Gaudreau, P.; Thelander, L.; Guindon, Y. Specific inhibition of ribonucleotide reductases by peptides corresponding to the C-terminal of their second subunit. *Biochem. Cell Biol.* **1991**, *69*, 79–83.
- (8) Filatov, D.; Ingemarson, R.; Graslund, A.; Thelander, L. The role of herpes simplex virus ribonucleotide reductase small subunit carboxyl terminus in subunit interaction and formation of iron-tyrosyl center structure. *J. Biol. Chem.* **1992**, *267*, 15816.
- (9) Gaudreau, P.; Paradis, H.; Langelier, Y.; Brazeau, P. Synthesis and inhibitory potency of peptides corresponding to the subunit 2 C-terminal region of herpes virus ribonucleotide reductase. *J. Med. Chem.* **1990**, *33*, 723–730.
- (10) Moss, N.; Déziel, R.; Adams, J.; Aubry, N.; Bailey, M.; Baillet, M.; Beaulieu, P.; DiMaio, J.; Ducepe, J.-S.; Ferland, J.-M.; Gauthier, J.; Ghio, E.; Goulet, S.; Grenier, L.; Lavallée, P.; Lépine-Frenette, C.; Plante, R.; Rakhit, S.; Soucy, F.; Wernic, D.; Guindon, Y. Inhibition of herpes simplex virus type 1 ribonucleotide reductase by substituted tetrapeptide derivatives. *J. Med. Chem.* **1993**, *36*, 3005–3009.
- (11) Moss, N.; Déziel, R.; Ferland, J.-M.; Goulet, S.; Jones, P.-J.; Leonard, S. F.; Pitner, T. P.; Plante, R. Herpes simplex virus ribonucleotide reductase subunit association inhibitors: the effect and conformation of  $\beta$ -alkylated aspartic acid derivatives. *Bioorg. Med. Chem.* **1994**, *2*, 959–970.
- (12) Chang, L. L.; Hannah, J.; Ashton, W. T.; Rasmussen, G. H.; Ikeler, T. J.; Patel, G. F.; Garsky, V.; Uncapher, C.; Yamanaka, G.; McClements, W. L.; Tolman, R. L. Substituted penta- and hexapeptides as potent inhibitors of herpes simplex virus type 2 ribonucleotide reductase. *Bioorg. Med. Chem. Lett.* **1992**, *2*, 1207–1212.
- (13) For examples of pertinent HIV protease inhibitors, see: (a) Kim, E. E.; et al. Crystal structure of HIV-1 protease in complex with VX-478, a potent and orally bioavailable inhibitor of the enzyme. *J. Am. Chem. Soc.* **1995**, *117*, 1181–1182. (b) Dorsey, B. D.; et al. L-735,524: The design of a potent and orally bioavailable HIV protease inhibitor. *J. Med. Chem.* **1994**, *37*, 3443–3451. (c) Lam, P. Y. S.; et al. Rational design of potent, bioavailable, nonpeptide cyclic ureas as HIV protease inhibitors. *Science* **1994**, *263*, 380–383. (d) Roberts, N. A.; et al. Rational design of peptide-based HIV proteinase inhibitors. *Science* **1990**, *248*, 358–361.
- (14) The IC<sub>50</sub>s of all the inhibitors discussed in this paper were determined by a radioligand binding assay, which measures the ability of inhibitors to compete with a radiolabeled inhibitor for binding to immobilized large subunit. Krogsrud, R. L.; Welchner, E.; Scouten, E.; Liuzzi, M. A solid-phase assay for the binding of peptidic subunit association inhibitors to the herpes simplex virus ribonucleotide reductase large subunit. *Anal. Biochem.* **1993**, *213*, 386–390.
- (15) The binding assay potencies of all the compounds in Table 3 are below 1 nM. The cell culture potency and structure of BILD 733 were first described in ref 3.
- (16) This observation has also been reported in ref 12.
- (17) Langlois, M.; Allard, J. P.; Nugier, F.; Aymard, M. A rapid and automated colorimetric assay for evaluating the sensitivity of herpes simplex strains to antiviral drugs. *J. Biol. Stand.* **1986**, *14*, 201–211.
- (18) Denizot, F.; Lang, R. Rapid colorimetric assay for cell growth and survival. Modifications to the tetrazolium dye procedure giving improved sensitivity and reliability. *J. Immunol. Methods* **1986**, *89*, 271–277.
- (19) Evans, D. A.; Takacs, J. M. Enantioselective alkylation of chiral enolates. *Tetrahedron Lett.* **1980**, *21*, 4233–4236.
- (20) Maxim, N. A. Sur l'acide dibenzylacétique et quelques amides dérivées. (Dibenzylacetic acid and various amide derivatives.) *Bull. Soc. Chim. Fr.* **1926**, *39*, 1024–1029.
- (21) Aboul-Enein, M. N.; Khalifa, M.; El-Difrawy, S.; Badr, M. Z. 1,3-Substituted 2,5-pyrrolidinediones as anti-inflammatory agents. *Pharm. Acta Helv.* **1980**, *55*, 50–53.
- (22) Maiti, S. M.; Singh, M. P.; Micetich, R. G. Facile conversion of azides to amines. *Tetrahedron Lett.* **1986**, *27*, 1423–1424.

JM950248C